

Holographic evaluation of warp in the torsion of a bar of cellular solid: effect of Cosserat elasticity

Anderson, W. B., Lakes, R. S., and Smith, M. C., "Holographic evaluation of warp in the torsion of a bar of cellular solid", *Cellular Polymers*, 14, 1-13, (1995).

Abstract

Holographic methods are utilized to examine deviations from classical elasticity in a cellular solid, polymethacrylamide closed cell foam. A square cross section bar is subjected to static torsional deformation. The warp deformation is observed to be less in a foam bar than in a homogeneous polymeric bar used as a control. The homogeneous bar obeys the predictions of classical elasticity. Behavior of the foam bar is consistent with Cosserat elasticity. In a Cosserat solid, points in the continuum to rotate as well as translate, and the material supports couple per unit area as well as force per unit area. Cosserat effects can lead to enhanced toughness.

Introduction

Cellular solids are two phase composite materials in which one phase is solid and the other is a fluid, most often air. If the size scale of the micro-structure becomes large enough, the material may no longer be assumed to be continuous. Some researchers have found that classical elasticity theory, currently used in engineering analyses of deformable objects at small strain, does not always adequately describe the behavior of cellular materials.

Other continuum theories for linear isotropic materials are available. Some have more freedom than classical elasticity. The various continuum theories are all mathematically self consistent. Therefore a discrimination among them is to be made by experiment. In *classical* elasticity, points in the continuum can undergo translation, and the continuum supports a force per unit area, or stress. The rigidity of circular cylindrical bars of diameter d in tension goes as d^2 ; in bending and torsion, the rigidity goes as d^4 . There is no length scale in classical elasticity. In Cosserat elasticity, there is a rotational degree of freedom of *points* in the continuum, and the possibility of a couple stress, or moment per unit area. In Cosserat solids, a size-effect is predicted in the torsion of circular cylinders of Cosserat elastic materials. Slender cylinders in torsion appear more stiff than expected classically (Gauthier and Jahsman, 1975); a similar size effect is also predicted in the bending of plates, and of beams (Krishna Reddy and Venkatasubramanian, 1978) No size effect is predicted in tension. The stress concentration factor for a circular hole, is smaller than the classical value, and small holes exhibit less stress concentration than larger ones (Mindlin, 1963). This phenomenon of stress redistribution can be expected to confer a measure of toughness upon Cosserat solids.

Physically, the couple stresses in Cosserat and microstructure elasticity represent spatial averages of distributed moments per unit area, just as the ordinary (force) stress represents a spatial average of force per unit area. In cellular solids moments may be transmitted through the cell ribs or walls. The Cosserat characteristic lengths are expected to be on the order of the size scales in the microstructure. In foams they may be sufficiently large to observe experimentally.

This study is directed at the deformation field in the case of torsion of a square cross section bar, and how it depends on material micro-structure. Interpretation of the results is aided by generalized continuum theory: Cosserat elasticity.

Materials and Methods

Torsion experiments were conducted upon square cross section bars of Rohacell® polymethacrylamide closed cell foam (grade WF 300, $\rho = 0.38 \text{ g/cm}^3$, Cyro Industries) and amorphous polymethyl methacrylate (PMMA) at room temperature. Both the Rohacell bar and the PMMA specimen were 16.6 mm in square cross section; the Rohacell was 135 mm long and the PMMA was 140 mm long. The PMMA, which is transparent, was painted white to obtain a diffusely reflecting surface. Each end of each specimen was cemented firmly on a precision rotation stage (Newport Corporation). The rotation stages were connected by steel rods parallel to the

specimen to provide torque reaction. Torsion was achieved by advancing the micrometer screws on each rotation stage so that the top and bottom of the specimen rotated in opposite directions. Twist per unit length was 0.071 rad/m giving rise to a predicted classical peak strain of 8×10^{-4} . The amount of rotation of the top and bottom rotation stages was chosen so that a region of zero angular displacement of the specimen was imaged near the center of the holographic film. The specimen and the holographic components were installed on a research grade damped table top supported upon four pneumatic isolation mounts (Newport Corporation). A light beam from a 15 milliwatt helium-neon laser was divided by a variable beamsplitter into an object beam and a reference beam. Image plane double exposure transmission holograms were made via a unity magnification configuration using a four element coated lens system. For the purpose of simplifying the calculation, the reference and reconstruction beams were collimated. Moreover the object illumination beam was directed at an oblique angle, 16.6° with respect to the specimen surface by a cube beamsplitter, as shown in Fig. 1. The reason for the oblique illumination is to obtain maximum sensitivity to the warping deformation, which is in the plane of the bar surface, in the direction of the bar axis. Each exposure was about three seconds, achieved using a digitally controlled shutter. Agfa 8E75 holographic film was used. The film was developed in Kodak D19 and bleached in ammonium dichromate bleach to increase the image brightness. The images were viewed and photographed in laser light of 633 nm wavelength, the same as was used for making the holograms. Since the fringes themselves have some depth, a sufficiently small aperture stop was used in the camera lens to achieve adequate resolution of the fringes. The photographic images were enlarged to 11" by 14", and the fringe deflection associated with warp was measured from the enlargements.

Fringe patterns obtained by double exposure holography represent a map of displacement in a direction specified by experimental conditions. The zero-order fringe method [see, e.g. Schumann and Dubas, 1979] was used for interpretation of the holographic fringe patterns. The relation between the displacement vector \mathbf{u} and the fringe order n at a point P on the illuminated surface of the specimen is given by

$$n = \mathbf{u} \cdot (\mathbf{k} - \mathbf{h}) \quad (1)$$

in which λ is the wavelength of the light, \mathbf{k} is the unit vector from the object to the observer's eye, and \mathbf{h} is the unit vector from the light source to the object. The angle required to determine \mathbf{h} was obtained from the length of a shadow cast by a test object upon the specimen. The angle required to determine \mathbf{k} was obtained from the change in spacing of black marks made upon the specimen surface.

Fringe patterns were evaluated via existing analytical solutions of the torsion problem for a square section bar in classical elasticity (see, e.g. Sokolnikoff, 1983) and in Cosserat elasticity (Park and Lakes (1987)). The warp does not depend on the shear modulus, but it does depend on the Cosserat characteristic lengths and coupling number as defined below. In a Cosserat solid the warp is reduced in comparison with the classical elastic value. As a result, surface strain does not vanish at the corner of the cross section and peak strain at the center of the lateral surface is reduced. The degree of warp was evaluated from the fringes as shown in Fig. 2, which shows a theoretical fringe pattern for a classical elastic material. Consider the vertical dotted line as the edge of the plane which does not rotate, that is, for which the displacements $u_x = u_y = 0$. Fringe deviations from this line are due to warp. The distance Δx is proportional to the slope of the warp curve at the center-line of the bar surface, based on Eq. 1 and the displacement field for torsion. Δx was measured on the fringe photographs, and the ratio of the Δx values for the PMMA and the foam was calculated and compared with the corresponding theoretical ratio for classical and Cosserat theories.

Analysis: Elasticity theories

Foams and other materials with micro-structure are not continuous media. However no material in the physical world is a continuum either, since all materials are composed of atoms. Analysis of material properties for engineering application is facilitated by the use of a continuum theory which allows the details of the micro-structure to be averaged. The continuum theories considered in this study are classical elasticity and Cosserat elasticity.

Classical Elasticity

The constitutive equation for *classical* isotropic elasticity (Sokolnikoff, 1983; Fung, 1968), is as follows, in which there are the two independent elastic constants λ and G , the Lamé constants.

$$\sigma_{kl} = \lambda \epsilon_{rr} \delta_{kl} + 2G \epsilon_{kl} \quad (2)$$

The Poisson's ratio $\nu = \lambda / 2(\lambda + G)$ is restricted by energy considerations to have values in the range from -1 to 1/2. There is no length scale in classical elasticity.

Cosserat (micropolar) Elasticity

The Cosserat theory of elasticity (Cosserat, 1909) incorporates a local rotation of *points* as well as the translation assumed in classical elasticity; and a couple stress (a torque per unit area) as well as the force stress (force per unit area). The force stress is referred to simply as 'stress' in classical elasticity in which there is no other kind of stress. Several authors developed the theory in the language of modern continuum mechanics (Aero and Kuvshinskii, 1960; Mindlin and Tiersten, 1962; Mindlin, 1965; Eringen, 1968; Nowacki, 1970). Eringen (1968) incorporated micro-inertia and renamed Cosserat elasticity *micropolar* elasticity. Here we use the terms Cosserat and micropolar interchangeably. In the isotropic Cosserat solid there are six elastic constants, in contrast to the classical elastic solid in which there are two, and the uniconstant material in which there is one. The constitutive equations for a linear isotropic Cosserat elastic solid are, in the symbols of Eringen, (1968):

$$\sigma_{kl} = \lambda \epsilon_{rr} \delta_{kl} + (2\mu + \gamma) \epsilon_{kl} + e_{klm} (r_{m,n} - r_{n,m}) \quad (3)$$

$$m_{kl} = \mu_{r,r} \delta_{kl} + \mu_{k,l} + \mu_{l,k} \quad (4)$$

The usual summation convention for repeated indices is used throughout, as is the comma convention representing differentiation with respect to the coordinates. σ_{kl} is the force stress, which is a symmetric tensor in equation 2 but it is asymmetric in Eq. 3. m_{kl} is the couple stress, $\epsilon_{kl} = (u_{k,l} + u_{l,k})/2$ is the small strain, u_k is the displacement, and e_{klm} is the permutation symbol. The microrotation θ_k in Cosserat elasticity is kinematically distinct from the macrorotation $\theta_k = (e_{klm} u_{m,l})/2$ obtained from the displacement gradient.

In three dimensions, the isotropic Cosserat elastic solid requires six elastic constants $\lambda, \mu, \gamma, \mu_1, \mu_2, \mu_3$ and μ_4 for its description. A comparison of symbols used by various authors was presented by Cowin (1970a). The following technical constants derived from the tensorial constants are beneficial in terms of physical insight. These are (Eringen, 1968; Gauthier and Jahsman, 1975):

Young's modulus $E = (2\mu + \gamma)(3\lambda + 2\mu + \gamma)/(2\lambda + 2\mu + \gamma)$

shear modulus $G = (2\mu + \gamma)/2$,

Poisson's ratio $\nu = \lambda / (2\lambda + 2\mu + \gamma)$

characteristic length for torsion $l_t = [(\lambda + \gamma)/(2\mu + \gamma)]^{1/2}$,

characteristic length for bending $l_b = [\lambda / 2(2\mu + \gamma)]^{1/2}$,

coupling number $N = [\lambda / 2(\mu + \gamma)]^{1/2}$, and

polar ratio $\nu_p = (\lambda + \gamma) / (\lambda + \mu + \gamma)$.

When μ_1, μ_2, μ_3 vanish, the solid becomes classically elastic. The case $N = 1$ (its upper bound) is known as 'couple stress theory' (Mindlin and Tiersten, 1962; Cowin, 1970b). This corresponds to $\nu_p = 1$, a situation which is permitted by energetic considerations, as is incompressibility in classical elasticity.

Discrimination among continuum representations

Analytical predictions of Cosserat characteristic lengths have been developed for a variety of structures. In cellular solids it may be comparable to the average cell size (Adomeit, 1967). In some cellular materials, the characteristic length can exceed the cell size, in contrast to theory which predicts it should be smaller. In fibrous composites, the characteristic length l may be the on the order of the spacing between fibers (Hlavacek, 1975). Structure, however, does not necessarily lead to Cosserat elastic effects. Composite materials containing elliptic or spherical inclusions are predicted to have a characteristic length of *zero* (Hlavacek, 1976; Berglund, 1982).

One may determine the appropriate continuum representation for a material by experiment. Cosserat elasticity manifests itself in size effects in the torsion and bending rigidity as reviewed in the Introduction. It is known that common engineering materials such as steel and aluminum behave classically (Ellis and Smith, 1968). Several materials have been demonstrated to behave as Cosserat solids: several foams (Lakes, 1983, 1986, as well as human bone, a natural composite (Yang and Lakes, 1982; Lakes and Yang, 1983; Park and Lakes, 1987).

Results and Discussion

Fringe patterns for PMMA and for the Rohacell foam are shown in Figures 4 and 5 respectively. The patterns disclose less warp in the Rohacell specimen than in the PMMA specimen. A computed fringe pattern for the PMMA based on classical elasticity is shown in Fig. 2. The calculated fringe deviation due to warp agrees with the observed value within 7%, equivalent to the limit of error associated with the breadth of the fringes.

In the Rohacell foam, the maximum excursion of the central fringe due to warp is 0.8 of the classical value. For comparison, a computed fringe pattern for the Rohacell foam based on Cosserat elasticity is shown in Fig. 3. Assumed elastic constants are the characteristic lengths $l_t = 0.8$ mm and $l_b = 0.77$ mm; and $\nu = 1.5$ based on the results of Anderson and Lakes (1994) obtained by measurements of size effects in the torsion and bending rigidity of bars. The warp for a given twist angle does not depend on the shear modulus of the material. The size effect study did not yield an accurate value for the coupling number N owing to the difficulty in preparing very slender specimens. The size effect data are consistent with values of N over a wide range, at least from 0.1 to 0.3. The warp results in the present study give a value $N = 0.07$. Assuming a 5% error in the zero order fringe deviation δ , a permissible interval for N is from 0.05 to 0.08. The value of N inferred in the present polymethacrylimide foam is less than the value $N = 0.2$ determined in prior studies of a polyurethane foam (Lakes 1986).

The fringes have a grainy character. In the case of the PMMA, this graininess is due to laser speckle. The size of the speckles depends inversely on the lens aperture of the camera used to photograph the holograms. The fringes obtained in the present geometry have some depth, therefore a relatively small camera aperture was necessary, giving rise to noticeable speckles. In the case of the Rohacell foam, the fringes are very lumpy. The reason is that deformation of foam materials is inhomogeneous [Chen and Lakes, 1991, 1993]. The lumpiness of the fringes becomes more pronounced at higher strain levels. Therefore it was not possible to improve use higher strain levels to obtain finer and more densely packed fringes, hence to achieve better resolution.

The present method of measuring displacements due to warp has the advantage of revealing the presence and degree of Cosserat elastic behavior from study of a single relatively large specimen. This is in contrast to the method of size effects, which involves rigidity measurements on a set of specimens of different diameter, the smallest of which should have a diameter as small as a few times the characteristic length. The disadvantage of the warp measurement is that it is not apparent how one could independently evaluate the six Cosserat elastic constants, as can be done with the method of size effects. The present method based on warp permits quantitative comparisons, in contrast to a screening method presented by (Lakes, et al, 1985). That holographic method disclosed qualitative evidence of non-classical deformation in the torsion of bars of materials with micro-structure. A notch was made in a corner of a twisted square section bar. The edges of the notch displace in a Cosserat solid, giving an easily visible fringe discontinuity which enables the observer to discriminate classical from Cosserat solids. Given the lack of a solution of the full analytical problem for the notched bar, quantitative interpretation is not possible.

Implications of the present results are as follows. The observed reduction in warp in the twisted bar of foam implies a redistribution of strain. The peak strain at the center of the lateral surfaces is reduced. Strain 'spills over' into the region near the corners of the cross section, where classically it should tend to zero toward the corners. This redistribution of strain should enhance toughness since peak strains are reduced. We remark that this redistribution effect is not taken into account by ad-hoc criteria for fracture used in composites (Whitney and Nuismer, 1974). In the

present polymethacrylimide foam, the effect is relatively small owing to the small value of N . If a material with a larger N were developed, we would expect it to exhibit enhanced toughness.

Conclusions

1. Warp in a bar of Rohacell foam under torsion is less than the value predicted by classical elasticity. By contrast, solid PMMA as a control exhibits warp consistent with classical elasticity.
2. Warp deformation predicted via Cosserat elasticity using elastic constants derived from prior size effect studies is in agreement with the present experimental results.

Acknowledgment

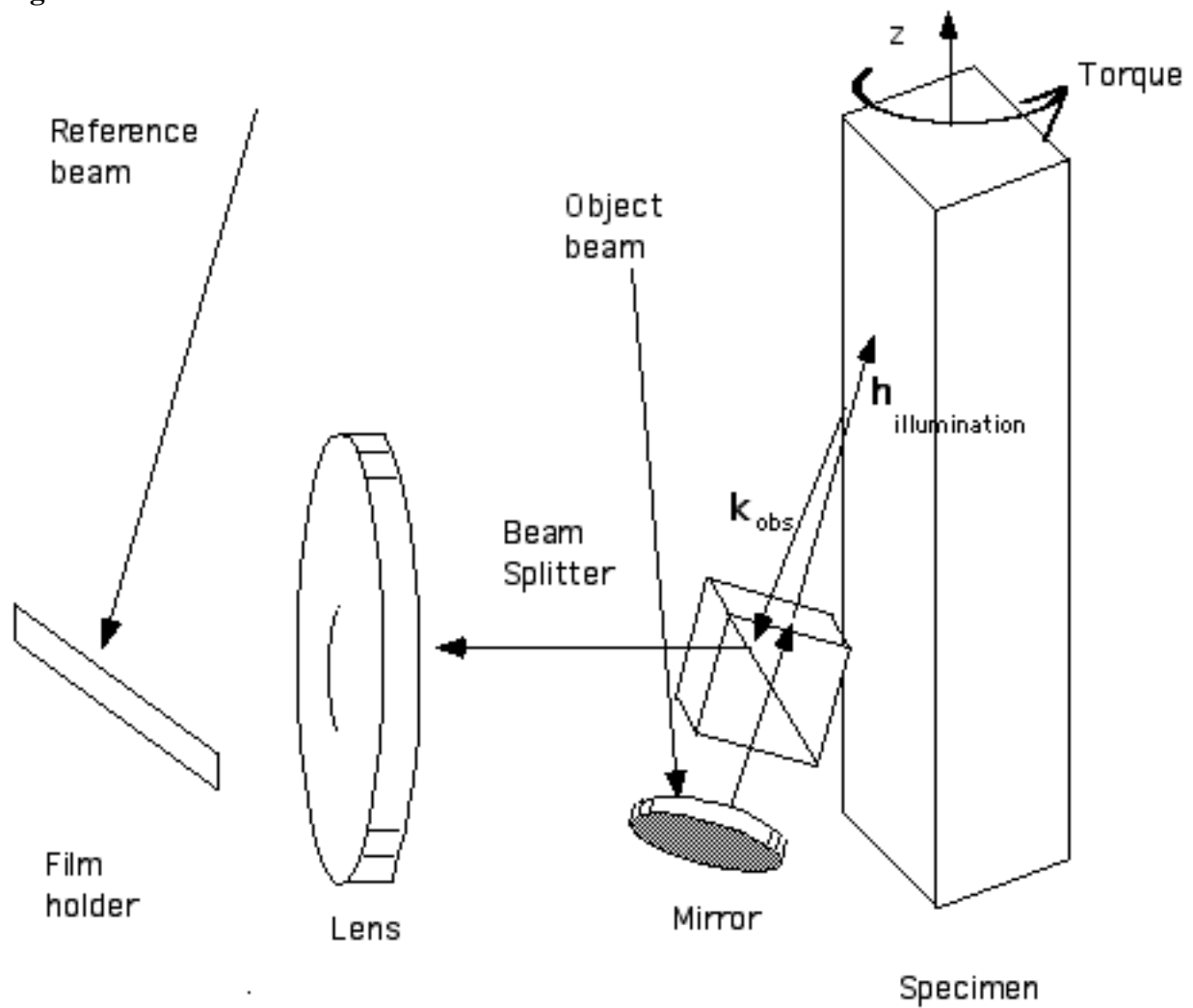
Partial support by the NASA/ Boeing ATCAS program is gratefully acknowledged.

References

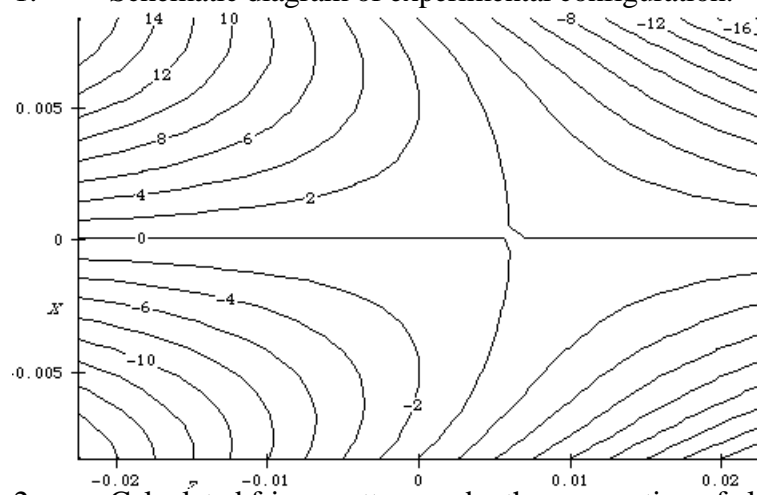
- Adomeit, G., "Determination of elastic constants of a structured material", *Mechanics of Generalized Continua*, (Edited by Kröner, E.), IUTAM Symposium, Freudenstadt, Stuttgart. Springer, Berlin, (1967).
- Aero, E. L. and Kuvshinskii, E. V., "Fundamental equations of the theory of elastic media with rotationally interacting particles", *Fizika Tverdogo Tela*, 2, 1399-1409, 1960; Translation, *Soviet Physics-Solid State* 2, 1272-1281, 1961.
- Anderson, W. B. and Lakes, R. S., "Size effects due to Cosserat elasticity and surface damage in closed-cell polymethacrylimide foam", *Journal of Materials Science*, 29, 6413-6419, (1994).
- Berglund, K., "Structural models of micropolar media", in *Mechanics of Micropolar Media*, edited by O. Brulin and R. K. T. Hsieh, World Scientific, Singapore, 1982.
- Brezny, R. and Green, D. J., "Characterization of edge effects in cellular materials", *J. Materials Science*, 25, 4571-4578, 1990.
- Chen, C.P. and Lakes, R.S., "Holographic study of conventional and negative Poisson's ratio metallic foams: elasticity, yield, and micro-deformation", *J. Materials Science*, 26, 5397-5402 (1991)
- Chen, C. P. and Lakes, R. S., "Holographic study of non-affine deformation in copper foam with a negative Poisson's ratio -0.8", *Scripta Metall et Mater.*, 29, 395-399, (1993).
- Cosserat, E. and Cosserat, F., *Theorie des Corps Deformables*, Hermann et Fils, Paris, 1909.
- Cowin, S. C., "Stress functions for Cosserat elasticity", *Int. J. Solids, Structures*, 6, 389-398, 1970.
- Cowin, S. C. "An incorrect inequality in micropolar elasticity theory." *J. Appl. Math. Phys. (ZAMP)* 21, 494-497, 1970b.
- Ellis, R.W. and Smith, C.W., "A thin plate analysis and experimental evaluation of couple stress effects", *Experimental Mechanics*, 7, 372-380, 1968.
- Eringen, A.C. Theory of micropolar elasticity. In *Fracture* Vol. 1, 621-729 (edited by H. Liebowitz), Academic Press, 1968.
- Fung, Y.C., *Foundations of Solid Mechanics*, Prentice Hall, 1968.
- Gauthier, R. D. and W. E. Jahsman. "A quest for micropolar elastic constants." *J. Applied Mechanics*, 42, 369-374, 1975.
- Hlavacek, M., "A continuum theory for fibre reinforced composites", *Int. J. Solids and Structures*, 11, 199-211, 1975.
- Hlavacek, M., "On the effective moduli of elastic composite materials", *Int. J. Solids and Structures*, 12, 655-670, 1976.
- Lakes, R. S. and Yang, J. F. C., "Micropolar elasticity in bone: rotation modulus ", Proceedings 18th Midwest Mechanics Conference, *Developments in Mechanics* 12, 239-242, 1983.
- Lakes, R. S. "Size effects and micromechanics of a porous solid." *J. Materials Science*, 18, 2572-2581, 1983.
- Lakes, R. S., D. Gorman and W. Bonfield. "Holographic screening method for microelastic solids." *J. Materials Science*, 20, 2882-2888, 1985.

- Lakes, R.S., "A pathological situation in micropolar elasticity, *J. Applied Mechanics*, 52 234-235 1985a.
- Lakes, R. S. "Demonstration of consequences of the continuum hypothesis." *Mechanics Monograph*, M5, 1-5, 1985b.
- Lakes, R. S., "Experimental microelasticity of two porous solids", *Int. J. Solids, Structures*, 22, 55-63, 1986.
- Mindlin, R. D. and Tiersten, H. F., "Effect of couple stresses in linear elasticity", *Arch. Rational Mech. Analy*, 11, 415-448, 1962.
- Mindlin, R. D., "Effect of couple stresses on stress concentrations", *Experimental Mechanics*, 3, 1-7, 1963.
- Mindlin, R. D., "Micro-structure in linear elasticity", *Arch. Rational Mech. Analy*, 16, 51-78, 1964.
- Mindlin, R. D., "Stress functions for a Cosserat continuum", *Int. J. Solids and Structures* 1, 265-271, 1965.
- Park, H. C. and R. S. Lakes. "Cosserat micromechanics of human bone: strain redistribution by a hydration-sensitive constituent." *J. Biomechanics*, 19, 385-397, 1986.
- Park, H. C. and R. S. Lakes. "Torsion of a micropolar elastic prism of square cross section." *Int. J. Solids, Structures*, 23, 485-503, 1987.
- Schumann, W. and Dubas, M., "Holographic interferometry" (Springer-Verlag, 1979), Berlin.
- Sokolnikoff, I.S., *Mathematical Theory of Elasticity*, Krieger, 1983.
- Whitney, J.M. and Nuismer, R.J., Stress fracture criteria for laminated composites containing stress concentrations, *J. Composite Materials*, 8, 253-275, 1974
- Yang, J. F. C. and R. S. Lakes. "Experimental study of micropolar and couple-stress elasticity in bone in bending." *J. Biomechanics*, 15, 91-98, 1982.

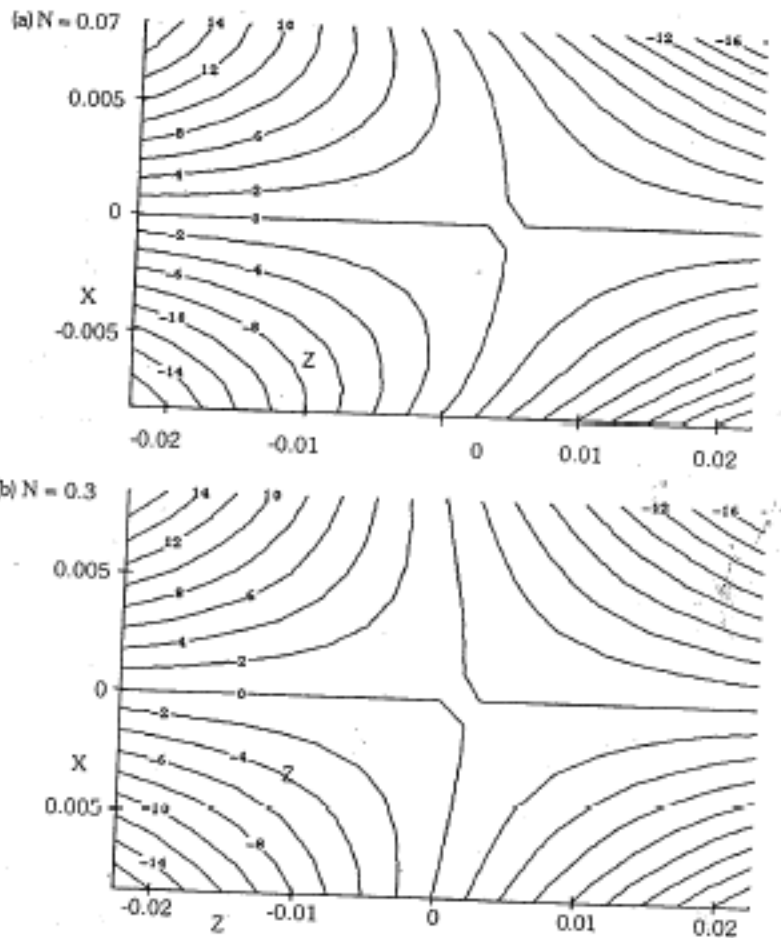
Figures



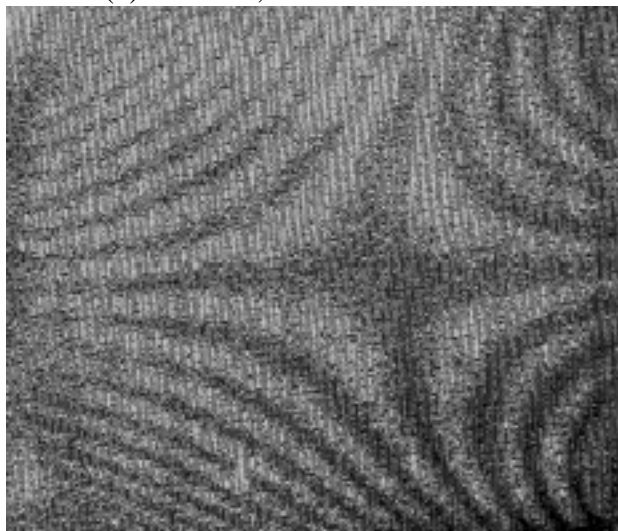
1. Schematic diagram of experimental configuration.



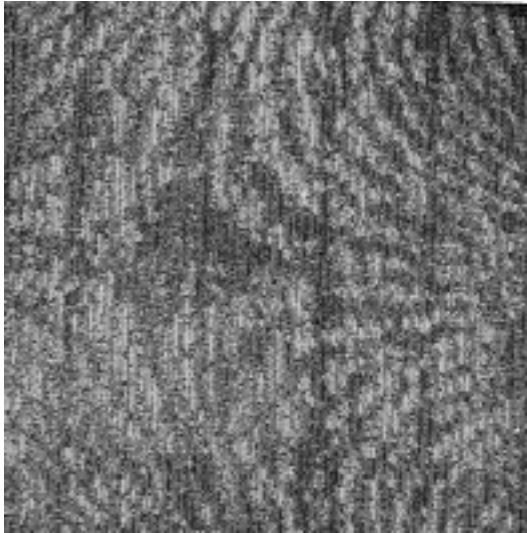
2. Calculated fringe pattern under the assumption of classical elasticity.



3. Calculated fringe pattern under the assumption of Cosserat elasticity.
 (a) $l_t = 0.8$ mm and $l_b = 0.77$ mm, $\nu = 1.5$ and $N = 0.07$.
 (b) as above, but $N = 0.3$



4. Holographic fringe pattern for torsion of a square section bar of PMMA.



5. Holographic fringe pattern for torsion of a square section bar of Rohacell polymethacrylimide foam.